

See discussions, stats, and author profiles for this publication at: <https://www.researchgate.net/publication/51085380>

Vibrational Properties of the Disulfur Dinitride Molecule, S₂N₂: IR and Raman Spectra of the Matrix-Isolated Molecule

ARTICLE *in* THE JOURNAL OF PHYSICAL CHEMISTRY A · MAY 2011

Impact Factor: 2.69 · DOI: 10.1021/jp202284b · Source: PubMed

CITATIONS

7

READS

135

4 AUTHORS, INCLUDING:



Anthony J Downs

University of Oxford

258 PUBLICATIONS 5,062 CITATIONS

SEE PROFILE



Ralf Koepp

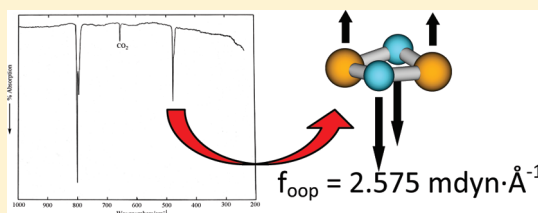
Karlsruhe Institute of Technology

128 PUBLICATIONS 1,452 CITATIONS

SEE PROFILE

Vibrational Properties of the Disulfur Dinitride Molecule, S_2N_2 : IR and Raman Spectra of the Matrix-Isolated Molecule[†]Richard Evans,[‡] Anthony J. Downs,^{*,‡} Ralf Köppe,[§] and Stephen C. Peake[‡][‡]Department of Inorganic Chemistry, University of Oxford, South Parks Road, Oxford, OX1 3QR, U.K.[§]Institut für Anorganische Chemie, Karlsruher Institut für Technologie, Engesserstrasse 15, D-76131 Karlsruhe, Germany Supporting Information

ABSTRACT: The IR and Raman spectra of disulfur dinitride, S_2N_2 , are reported not only for the solid condensate but also for the molecules isolated in solid noble gas, N_2 , or CH_4 matrices at low temperatures. The results imply that the isolated S_2N_2 molecule has much the same geometry as in the crystalline solid with a virtually square-planar structure conforming to D_{2h} symmetry, a conclusion confirmed by isotopic enrichment in ^{15}N and by the results of earlier as well as fresh quantum chemical calculations. These calculations also support the results of normal coordinate analysis of the experimental data in giving potential constants suggestive of a relatively rigid S_2N_2 molecule consistent with its description as a 2π -electron aromatic, while appearing to maintain a formal S–N bond order close to 1.



1. INTRODUCTION

First characterized more than 50 years ago by Goehring and Voigt¹ as a product of the thermal decomposition of tetrasulfur tetranitride, S_4N_4 , disulfur dinitride, S_2N_2 , is a compound of no little interest.^{2–4} Detailed studies have been severely limited by its properties, for it is liable to explode violently at temperatures exceeding 30 °C and is shock-sensitive. Somewhat more stable are the adducts it forms by coordination through one or both the N atoms to selected Lewis acids, e.g., $S_2N_2 \cdot BCl_3$ and $S_2N_2 \cdot 2SbCl_5$.^{4,5} X-ray studies of a single crystal of disulfur dinitride held at –130 °C reveal more or less discrete S_2N_2 molecules that are virtually square planar [angles S–N–S = 90.42(6)° and N–S–N = 89.58(6)° and essentially equal S–N bond lengths of 1.657(1) and 1.651(1) Å].⁶ The same structure is maintained with a modest attenuation of the S–N bonds in the crystalline adduct $S_2N_2 \cdot 2SbCl_5$.⁵ Very recent voltametric experiments with S_2N_2 in solution give evidence of reduction to the radical anion $[S_4N_4]^{•-}$ (probably via coupling of $[S_2N_2]^{•-}$ with S_2N_2), this decomposing in turn to $[S_3N_3]^-$; in the presence of moisture or with added HBF_4 , a longer lived radical $S_2N_2H^\bullet$ can be detected.

Two aspects of disulfur dinitride are of particular note: (i) The solid undergoes thermally or photolytically induced polymerization at low temperatures to form polythiazyl, $[SN]_x$, where the SN units are linked head-to-tail in planar quasi-one-dimensional chains.^{6,8} Polythiazyl has been something of a cause célèbre for its metallic properties, exhibiting good electrical conductivity along the chains and even becoming superconducting near 0.3 K. Various studies have probed both the electronic structure of polythiazyl⁹ and the mechanism of the polymerization process.¹⁰ While practical applications of the polymer have remained largely elusive, the polymerization process starting from S_2N_2 vapor has

been shown to offer a means of imaging fingerprints and inkjet traces.¹¹ (ii) There is, second, the question of the bonding in S_2N_2 . It was first described with four localized σ -bonds and six delocalized π -electrons, in accordance with the Hückel $4n + 2$ rule.^{10a,12} Numerous theoretical studies seeking to elucidate the structure have found difficulty, however, in arriving at a clear consensus. Thus, the aromaticity implicit in the earliest models has been countered by the resemblance of the primary Lewis-type valence bond (VB) structure to a spin-paired diradical with a long transannular $N \cdots N$ bond.¹³ Yet, while favoring a singlet diradical description, spin-coupled VB theory calculations lend weight to the contrary view that the diradical character is associated solely with two coupled π -electrons, one from each of the S atoms.¹⁴ More recently, though, various ab initio and DFT calculations have been used to re-establish the case for aromaticity. In common with the currently unknown analogues Se_2N_2 and $SeSN_2$,^{15–17} S_2N_2 should now be described, according to the most recent analysis,¹⁷ as a 2π -electron aromatic with minor singlet diradical character of 6–8% that can be attributed solely to the N atoms. High-level quantum chemical calculations have then been used to reproduce molecular properties for the S_2N_2 molecule close to those determined experimentally for the crystalline solid.^{6,17}

About the free S_2N_2 molecule unconstrained by intermolecular forces we have few experimental details. IR spectra have been measured under a variety of conditions.^{18,19} The IR spectrum of the vapor in the range 260–5000 cm^{-1} (recorded with the aid of a long-path cell)¹⁸ has been reported to display

Received: March 10, 2011

Revised: April 13, 2011

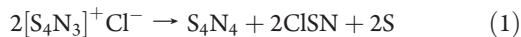
Published: April 29, 2011

two distinct absorptions (at 791 and 474.5 cm^{-1}) with the possibility of a third very weak feature (at 652 cm^{-1}). The photoelectron spectrum of the vapor under He–I and He–II irradiation has also been reported.²⁰ Microwave measurements are ruled out by a structure which apparently lacks a dipole moment, and gas-phase electron diffraction has been effectively precluded so far by the low vapor pressure of the compound at ambient temperatures (<1 Torr at 15 °C) and the serious risk of explosion when the temperature is raised.

Here we describe the results of some experiments in which S_2N_2 vapor has been trapped in a solid noble gas, N_2 , or CH_4 matrix at low temperatures. Hence both the IR and Raman spectra of isotopically natural and ^{15}N -enriched S_2N_2 have been measured, thereby enabling virtually all the vibrational fundamentals to be identified. The assignment of the spectra is supported by the results of earlier as well as fresh quantum chemical calculations. Normal coordinate analysis gives force constants consistent with a cyclic planar structure that is relatively rigid, i.e., in keeping with its having significant aromatic character. The vibrational properties are compared with those (i) of related molecules containing S–N bonds, and (ii) of other molecules having four-membered cyclic structures but two fewer valence electrons, e.g. M_2O_2 ($\text{M} = \text{Si}$ or Ge), P_2N_2 , and Al_2Cl_2 .

2. EXPERIMENTAL AND COMPUTATIONAL DETAILS

Experimental Details. Disulfur dinitride, S_2N_2 , was produced in situ from tetrasulfur tetranitride, S_4N_4 . The latter was prepared from disulfur dichloride, S_2Cl_2 , and ammonium chloride (BDH) following the method of Jolly and Becke-Goehring.²¹ For both the IR and Raman experiments, a two-stage Pyrex glass furnace was used to generate S_2N_2 by controlled pyrolysis of S_4N_4 vapor (formed by vaporization of the solid at 70–75 °C) on a column packed with silver wool (Johnson Matthey) and maintained at a temperature of 180–200 °C.²² In some experiments—and particularly those involving ^{15}N -enrichment of the samples—it was expedient also to form the S_4N_4 in situ by carefully controlled pyrolysis of solid $[\text{S}_4\text{N}_3]^+\text{Cl}^-$, which proceeds in accordance with eq 1.²³



S_2N_2 was then formed by passing the volatile products of this reaction occurring at 95–100 °C over heated silver wool at 180–200 °C, again by means of a two-stage Pyrex glass furnace. Use of $[\text{S}_4\text{N}_3]^+\text{Cl}^-$ offered the important advantage of a precursor that could be synthesized on a small scale relatively efficiently from NH_4Cl and S_2Cl_2 by way of $\text{S}_3\text{N}_2\text{Cl}_2$ following the method described by Logan and Jolly.²⁴ For the production of ^{15}N -enriched samples of S_2N_2 , NH_4Cl (1.0 g, Prochem, 30 or 95 atom % ^{15}N) and redistilled S_2Cl_2 (3.4 g, BDH) were typically used to prepare 0.5 g of $[\text{S}_4\text{N}_3]^+\text{Cl}^-$, representing a yield of about 40% based on the amount of NH_4Cl taken.

The furnace was coupled directly to the matrix-isolation or other cryogenic assembly so that the vapor effusing from the nozzle had direct access to a cooled CsI or Si window (for IR measurements) or a polished high-purity copper block (for Raman measurements). Some experiments exploited liquid nitrogen as the coolant, giving a substrate temperature near 77 K. Usually, however, this temperature was controlled in the range 15–35 K by means of either a two-stage Joule-Thomson refrigerator (Air Products model AC-2-109 “Cryotip”) in early IR experiments

or a closed-cycle refrigerator (Air Products “Displex” model CSA-202) in later IR and Raman experiments. Much trial and error was needed to secure the optimum conditions for the isolation of S_2N_2 with minimal contamination by unchanged S_4N_4 or other sulfur–nitrogen compounds formed in primary or secondary reactions, e.g., ClSN or S_4N_2 . Pressures within the matrix assembly were <10^{−6} Torr, while temperatures were monitored with a chromel vs iron-doped gold thermocouple. Fuller details of the matrix-isolation apparatus are given elsewhere.^{23,25,26}

The S_2N_2 vapor was caused to condense either alone or in admixture with a large excess of matrix gas (Ar, Kr, Xe, N_2 , or CH_4 , all British Oxygen, grade “X”). Matrix ratios (matrix gas: S_2N_2) were estimated typically to be on the order of 800:1, with the matrix gas being deposited at a rate of 2 mmol h^{−1} for a total time of 2–3 h.

The Raman spectra of the solid deposits, which varied in color from pale yellow to near-white, were measured initially with a Cary 81 spectrophotometer modified for use with laser-excitation and for analysis of the light scattered at 90° to the direction of the incident radiation. Later experiments deployed a Spex Ramalog 5 spectrophotometer with photon-counting detection; this instrument was equipped with a third monochromator, an additional facility that afforded a marked enhancement in spectral quality at low vibrational wavenumbers. The spectra were excited by the output from either a Spectra Physics model 125 He–Ne laser ($\lambda = 632.8$ nm) or a Spectra Physics model 165 Ar⁺ laser ($\lambda = 514.5$ nm). The wavenumbers of the Raman lines were calibrated by interpolation between the atomic emission lines of a low-pressure Ne discharge lamp superimposed on the spectrum. Spectra were recorded under optimum conditions with a resolution of 2 cm^{-1} and the wavenumbers of sharp lines could be measured reproducibly to within ± 1 cm^{-1} .

IR spectra of the deposits were recorded in transmission in the range 4000–200 cm^{-1} with a Perkin-Elmer model 225 spectrophotometer and in the range 800–70 cm^{-1} with a Beckmann IR 11 instrument, the sample chambers of both being purged with dry air. Calibration of the spectra was accomplished by reference to the positions of sharp lines in the vibrational–rotational spectrum of atmospheric H_2O and CO_2 ; in favorable circumstances, a wavenumber accuracy of ± 0.2 cm^{-1} could be achieved.

Calculations. *Quantum Chemical Calculations.* Intensive theoretical research was performed at different levels of theory with the aim of understanding the electronic nature of S_2N_2 despite the comparative lack of experimental data. On the basis of high-level calculations performed previously by different groups^{15–17} and of extensions of these to obtain vibrational frequencies of different isotopomers of S_2N_2 , we found that our experimental vibrational data are best matched by calculations using density functional theory (DFT). The geometry of S_2N_2 was calculated with D_{2h} symmetry at the B3LYP hybrid level²⁷ using a 6-311G++(3df,3pd) basis set for each atom. To compare the bonding situation in S_2N_2 with that in each of the analogous molecules Si_2O_2 , Ge_2O_2 , P_2N_2 , and Al_2Cl_2 , quantum chemical calculations were performed using the same level of theory and def2-TZVP basis sets²⁸ for each atom. Atomic charges in these molecules were gauged by means of population analyses based on occupation numbers (Ahlrichs–Heinzmann population analysis).²⁹ The values for atomic charge, Q , are made comparable by the application of minimal basis sets called modified atomic orbitals (MAOs). The number of MAOs chosen was 5 for O; 8 for Al; 9 for Si, P, S, and Cl; and 18 for Ge. Calculations were also carried out on HSN, SNH, *trans*- H_2NSH , and S_4N_4 to

Table 1. Symmetry Coordinates and Symmetrized F and G Matrix Elements for S₂N₂

symmetry coordinates	symmetrized matrix elements	
	F ^a	G
$S_1(a_g) = 1/2(\Delta r_1 + \Delta r_2 + \Delta r_3 + \Delta r_4)$	$F_{11} = f_r + f_{rr} + f_{rr}' + f_{rr}''$	$G_{11} = \mu_N + \mu_S + (\mu_N - \mu_S)\cos\alpha$
$S_2(a_g) = 1/2\Delta R$	$F_{22} = f_R$	$G_{22} = 2\mu_N$
	$F_{21} = 2f_{rR}$	$G_{12} = 2\mu_N\cos(\alpha/2)$
$S_3(b_{1g}) = 1/2(\Delta r_1 - \Delta r_2 + \Delta r_3 - \Delta r_4)$	$F_{33} = f_r - f_{rr} - f_{rr}' + f_{rr}''$	$G_{33} = \mu_N + \mu_S - (\mu_N - \mu_S)\cos\alpha$
$S_4(b_{1u}) = 1/2(\Delta z_1 - \Delta z_2 + \Delta z_3 - \Delta z_4)$	$F_{44} = f_{oop}$	$G_{44} = 1/2(\mu_N + \mu_S)$
$S_5(b_{2u}) = 1/2(\Delta r_1 - \Delta r_2 - \Delta r_3 + \Delta r_4)$	$F_{55} = f_r + f_{rr} - f_{rr}' - f_{rr}''$	$G_{55} = (\mu_N + \mu_S)(1 + \cos\alpha)$
$S_6(b_{3u}) = 1/2(\Delta r_1 + \Delta r_2 - \Delta r_3 - \Delta r_4)$	$F_{66} = f_r - f_{rr} + f_{rr}' - f_{rr}''$	$G_{66} = (\mu_N + \mu_S)(1 - \cos\alpha)$

^a f_{rr} relates to the interaction through a common N atom, f_{rr}' to that through a common S atom, and f_{rr}'' to that between opposite sides of the ring.

Table 2. Vibrational Wavenumbers (in cm⁻¹) and Relative Intensities^a Calculated for S₂¹⁴N₂ at Different Levels of Theory

mode	ab initio coupled cluster CASPT2 method ^b	DFT				expt IR and Raman spectra for Ar matrix
		PBE0 functional ^b	B3LYP functional ^c	B3LYP/6-311G+ + (3df, 3pd) functional ^d	PBE0 functional ^c	
$\nu_1(a_g)$	924 [0,−]	974 [0,100]	938	945	984.7 [0,100]	934
$\nu_2(a_g)$	648 [0,−]	662 [0,30]	643	650	665.6 [0,48]	617
$\nu_3(b_{1g})$	914 [0,−]	970 [0,38]	922	926	970.0 [0,53]	889
$\nu_4(b_{1u})$	476 [69,0]	490 [53,0]	477	483	497.3 [45,0]	473.7
$\nu_5(b_{2u})$	687 [28,0]	699 [2,0]	650	652	697.6 [2,0]	ca. 660
$\nu_6(b_{3u})$	790 [100,0]	840 [100,0]	777	795	853.8 [100,0]	789.2

^a Intensities given in brackets relative to the most intense absorption or scattering in the order [IR,Raman]. ^b Reference 17. ^c Reference 36. ^d Reference 37. ^e This research.

estimate structural and vibrational properties for other small molecules with different types of S–N bond.

All these calculations employed the program package TURBOMOLE.³⁰ Vibrational frequency calculations related to the optimized structure of each molecule at this level of theory via diagonalization of the analytically computed Hessian using the module AOFORCE.³¹ For better comparison of the theoretical force constant data with those derived from experimental vibrational spectra, each calculated force constant matrix expressed in the basis system of Cartesian coordinates was transformed into a system of appropriate symmetry coordinates using the program FCT³² (Table 1).

Normal Coordinate Analysis. The basis system of symmetry coordinates given in Table 1 describing a D_{2h} -type molecule X_2Y_2 (S₂N₂, Si₂O₂, Ge₂O₂, P₂N₂ and Al₂Cl₂) has been chosen to simplify a normal coordinate analysis based on experimental data. Except for the two totally symmetric a_g vibrations of such a molecule, each of the other normal vibrations belongs to a different symmetry species. An interaction force constant has therefore to be determined only for the two a_g vibrations. Following a proposal by Lesiecki and Nibler for Tl₂F₂ and Tl₂Cl₂,³³ we define the distance R between two X atoms in the ring (X = N, N, O, O, or Cl for S₂N₂, P₂N₂, Si₂O₂, Ge₂O₂, or Al₂Cl₂, respectively) as an unusual internal coordinate. With the chosen set of internal coordinates a set of symmetry coordinates free from redundancies can be generated. For the unique out-of-plane bending mode, the formulation of the G matrix element as $G_{44} = 1/2(\mu_S + \mu_N)$ was the best choice. The resulting G and F matrix elements and the relations between symmetry and internal force constants are summarized in Table 1. Normal coordinate analyses on S₂N₂ were performed by means of the program ASYM40.³⁴

3. RESULTS

Quantum Chemical Calculations. In the absence of any definitive experimental results, we are bound to rely on quantum chemical calculations to reproduce the geometry and other properties of the free S₂N₂ molecule. Notwithstanding arguments about the detailed electronic description,^{12–17} there is general agreement that the ground electronic state is a singlet with a near square-planar geometry of alternating S and N atoms conforming to D_{2h} symmetry. It is thus quite different from [NO]₂, which is a van der Waals dimer in which the NO units, only lightly perturbed, are linked through a weak N···N bond.^{25,35} According to the most recent calculations based on coupled cluster CASPT2 and DFT PBE0 methods,¹⁷ the S₂N₂ molecule features the following dimensions: $r(S-N) = 1.642-1.656$ Å, $\angle S-N-S = 88.7^\circ-89.1^\circ$, and $\angle N-S-N = 90.9^\circ-91.3^\circ$. The six vibrational fundamentals of such a molecule span the representation $2a_g + 1b_{1g} + 1b_{1u} + 1b_{2u} + 1b_{3u}$ with three of these modes ($2a_g + 1b_{1g}$) being active only in Raman scattering and the other three ($1b_{1u} + 1b_{2u} + 1b_{3u}$) active only in IR absorption. CASPT2 and PBE0 methods have been used¹⁷ to calculate the harmonic vibrational frequencies and IR/Raman intensities listed in Table 2, which also includes other estimates of the frequencies based on independent DFT calculations.^{36,37}

We too have performed calculations on S₂N₂ using the PBE0 functional in DFT methods with basis sets of def2-TZVP quality to arrive at a very similar geometry [$r(S-N) = 1.638$ Å, $\angle S-N-S = 88.9^\circ$, and $\angle N-S-N = 91.1^\circ$] and vibrational properties (see Table 2) close to those reported earlier.¹⁷ Hence we are led to expect a Raman spectrum consisting of three

Table 3. IR Spectrum of S₂N₂ in the Solid, Vapor, and Matrix-Isolated States (wavenumbers in cm⁻¹)^a

solid				matrix at 20 K ^d				assignment
at 80 K ^b	at 193 K ^c	annealed, at 77 K ^d	vapor ^b	Ar	Kr	Xe	N ₂	
795 vs	785 vs	793 vs	791 mw	789.2 s ^e 785.5 mw	790.3 s 788.6 w 787.0 w	787.3 s 785.4 m 781.7 w	794.8 s 791.8 m	ν_6 (b _{3u})
663 m	665 s	660 s	652 vvw?					ν_5 (b _{2u})
474 ms	476 s	474 ms	474.5 mw	473.7 ms ^e	473.0 ms	473.7 ms	476.1 ms	ν_4 (b _{1u})
	221.5 ms	232 m						
	90.9 m	86 mw						

^a Intensities: s, strong; m, medium; w, weak; v, very. ^b Reference 18. ^c Reference 19. ^d This research. ^e Wavenumbers (in cm⁻¹) of the corresponding bands for S₂¹⁵N₂, 770.4 and 461.6, and for S₂¹⁴N¹⁵N, 779.2 and 467.7.

emissions all of significant intensity with wavenumbers on the order of 950, 940, and 650 cm⁻¹, and an IR spectrum also consisting of three features but this time near 810, 680, and 480 cm⁻¹. The middle IR absorption (near 680 cm⁻¹) is predicted to be appreciably weaker than the other two, the DFT calculations suggesting an intensity 2 orders of magnitude smaller than that of the strongest absorption (near 810 cm⁻¹).

IR Measurements. The IR spectrum of an annealed, polycrystalline film of S₂N₂ displayed absorptions at 793, 660.5, 474, 232, and 86 cm⁻¹, all of which exhibited a common growth pattern, the most intense feature being that at 793 cm⁻¹ (see Table 3). Similar results have been reported in earlier studies.^{18,19} Depending on the precise conditions of pyrolysis, the spectrum was liable to show other bands of variable intensity. Most prominent were features at 932, 726/705, 554, and 346 cm⁻¹, also having a common origin and which could be recognized as arising from the presence of unchanged S₄N₄.^{19,26d,38} Other weak bands observed for some samples could be attributed to S₄N₂,³⁹ a potential byproduct of the pyrolysis of S₄N₄, and in the case of samples prepared from [S₄N₃]Cl, [ClSN]_n (*n* = 1 or 3).²³

When S₂N₂ vapor was first quenched on a window at 20 or 77 K, the resulting amorphous condensate exhibited only two of the IR absorptions characteristic of the crystalline solid, viz., those near 790 and 470 cm⁻¹. Gradual annealing of the solid to temperatures above 100 K was marked by the growth of the other three bands associated with the crystalline material. At temperatures above 235 K, all five bands were observed to decay with the concomitant growth of new bands attributable to either S₄N₄^{19,26d,38} or polythiazyl, [SN]_x.⁴⁰

The IR spectrum of the solid matrix formed by codepositing S₂N₂ vapor with a large excess of Ar, Kr, Xe, or N₂ at 20 K resembled closely that of the neat compound after rapid quenching of the vapor, consisting of a strong band near 790 cm⁻¹ and a second band of medium intensity near 470 cm⁻¹. The main difference from the spectrum of the neat solid was the pronounced sharpening of the bands. To lower wavenumber of the feature near 790 cm⁻¹ we observed one or two weak satellites. The single satellite with an intensity about 10% that of the main absorption exhibited by an Ar matrix could be attributed to the corresponding mode of the isotopomer ³²S³⁴S¹⁴N₂ (having a natural abundance of 9.9%). On the other hand, the intensities and wavenumbers of the satellites for Kr, Xe, and N₂ matrices suggested that matrix site effects were the predominant influence. Otherwise the spectrum showed on occasion weak features attributable to traces of S₄N₄^{19,26d,38} and ClSN²³ and more commonly ones originating in H₂O⁴¹ and CO₂⁴² impurities

that could be kept to a minimum but never wholly eliminated (see, for example, Figure 1a). Figure 1b shows how the spectrum responded to the isolation of a sample of S₂N₂ vapor that was 30 atom % enriched in ¹⁵N. Each of the bands was now seen to appear as a triplet with components more or less evenly spaced and approximating to the expected intensity pattern of 5:4:1. The wavenumbers of the components due to the isotopomers S₂¹⁴N¹⁵N and S₂¹⁵N₂ are listed in a footnote to Table 3.

Raman Spectra. The Raman spectrum of a solid S₂N₂ film deposited on the surface of a copper block held at 20 K is illustrated in Figure 2. It reveals just three prominent lines centered at 924, 884, and 608 cm⁻¹ (see Table 4). Depending on the efficiency of pyrolysis, the condensate produced in some experiments displayed additional weak bands at 720, 556, 346, and 198 cm⁻¹ having a common origin in unchanged S₄N₄.^{26d,38} Annealing the solid at temperatures up to ca. 230 K had but little effect on the spectrum beyond minor changes of band shape and wavenumber. Above this temperature, however, the three bands decayed as the deposit gradually transformed into a poorly scattering yellow-black solid. Removal, workup, and analysis of this solid disclosed once again, on the evidence of the IR and Raman spectra, the presence of both S₄N₄^{19,26d,38} and [SN]_x.⁴⁰

Much the same Raman spectrum was observed for an Ar, Kr, N₂, or CH₄ matrix doped with S₂N₂ vapor differing only slightly in the wavenumbers of the emissions, albeit substantially in their much reduced linewidths. The relevant details are included in Table 4 and a typical spectrum is illustrated in Figure 2b. Attempts to measure depolarization ratios were usually frustrated by the strongly scattering behavior of the matrices. With N₂ and CH₄, however, it was possible to form relatively transparent matrices and, as illustrated in Figure 2b for an N₂ matrix, depolarization ratios, ρ , significantly less than 0.75 were then observed for the scattering near 930 and 610 cm⁻¹ but not for that near 890 cm⁻¹. The first two bands were thus identified as arising from totally symmetric (a_g) vibrations, as matrix scattering could lead only to an increase in the observed value of ρ . Experiments in which S₂N₂ 30 atom % enriched in ¹⁵N was trapped in an Ar matrix failed to give any useful additional information, as it was impossible clearly to discern the features due to the different isotopomers S₂¹⁴N₂, S₂¹⁴N¹⁵N, and S₂¹⁵N₂. Starting from [S₄N₃]Cl 95 atom % enriched in ¹⁵N, experiments were therefore carried out with S₂¹⁵N₂ as the predominant vapor species. The Raman spectrum of this trapped in an Ar matrix showed the usual pattern of three bands but shifted relative to those at 934, 889, and 617 cm⁻¹ associated with S₂¹⁴N₂ under

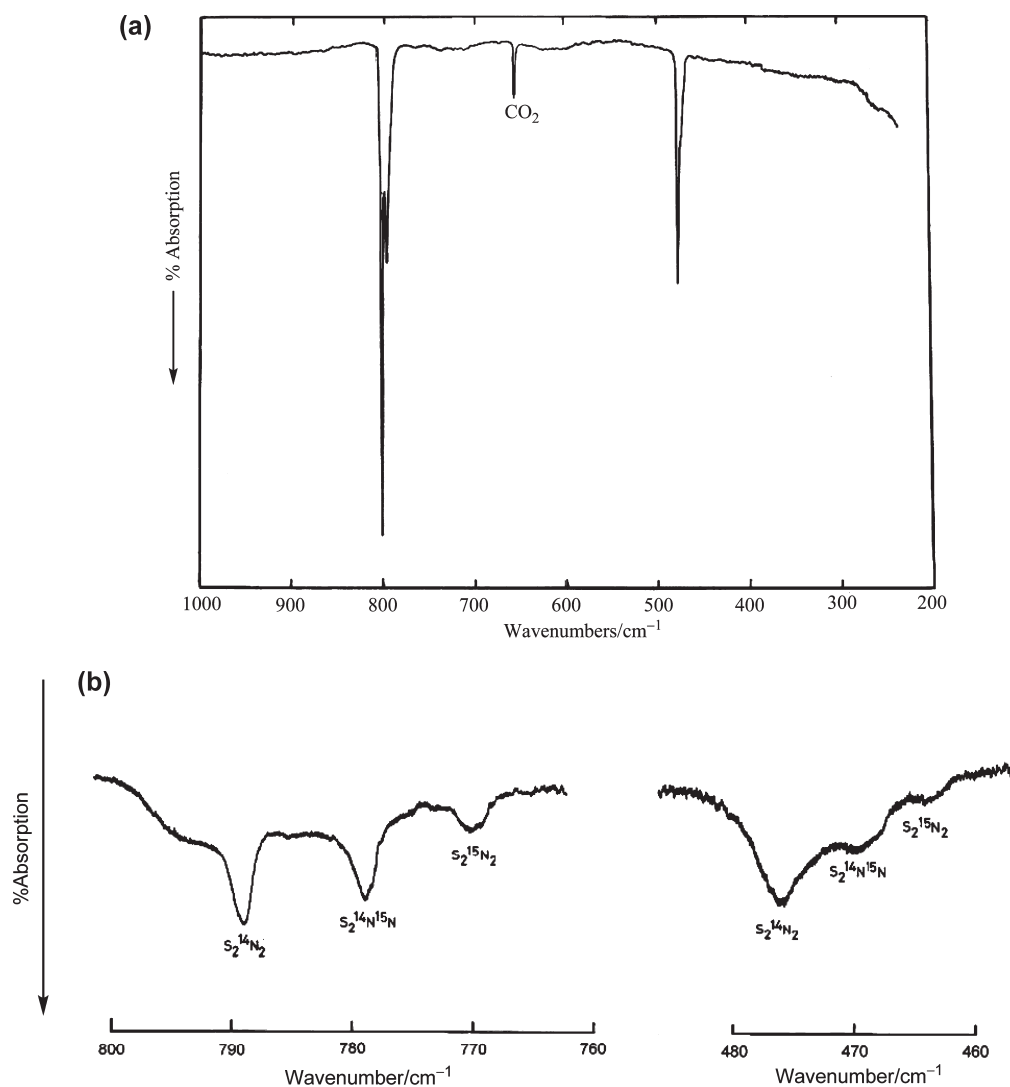


Figure 1. (a) IR spectrum of an Ar matrix doped with S_2N_2 . (b) Portions of the IR spectrum of an Ar matrix doped with S_2N_2 30% enriched in ^{15}N .

comparable conditions by -32 , -21 , and 0 cm^{-1} , respectively (see Table 4).

4. DISCUSSION

The simplicity of the IR and Raman spectra attributable to the S_2N_2 molecule and the lack of coincidences between the two are wholly consistent with a centrosymmetric geometry of D_{2h} symmetry. The observed bands may then be assigned on the evidence of (i) the selection rules that appear to operate, (ii) the wavenumbers, (iii) the polarization properties of the Raman bands, and (iv) the forecasts of earlier^{17,36,37} and fresh quantum chemical calculations as regards both the wavenumbers of the most abundant naturally occurring isotopomer and the wavenumber shifts occasioned by isotopic substitution of either ^{15}N or ^{34}S .

The interpretation of the Raman spectrum is made straightforward by the identification of the two a_g fundamentals with the scattering near 930 and 610 cm^{-1} , leaving the remaining signal near 890 cm^{-1} as the obvious candidate for the b_{1g} $\nu(S-N)$ mode, ν_3 . Strong support for the assignment comes not only from the results of the polarization measurements made on an N_2

matrix but also from the close agreement between the experimental and calculated wavenumber shifts brought about by the switch from $S_2^{14}N_2$ to $S_2^{15}N_2$ (see Table 5).

The two IR absorptions observed at 789.2 and 473.7 cm^{-1} for S_2N_2 isolated in an Ar matrix are most plausibly ascribed to the b_{3u} $\nu(S-N)$ (ν_6) and b_{1u} out-of-plane deformation (ν_4), respectively. This assignment is supported not only by the results of theoretical calculations but also by the contours of the IR bands reported for the vapor of the compound.¹⁸ The measured effects of ^{15}N or ^{34}S substitution, as revealed for S_2N_2 isolated in an Ar matrix, are also well-reproduced by the results of DFT calculations (see Table 5). Apparently missing from the measured spectra is any clear sign of the other IR-active $\nu(S-N)$ mode, ν_5 (b_{2u}). This is expected to appear in the neighborhood of 680 cm^{-1} . In their studies of S_2N_2 vapor,¹⁸ Warn and Chapman did observe a very weak absorption at 652 cm^{-1} which might correspond to this mode, but the result was not reproducible. Our studies of S_2N_2 -doped matrices were complicated in this region of the IR spectra by the presence of a weak band due to the ν_2 fundamental of CO_2 that occurred near 660 cm^{-1} . That the primary source of this band was CO_2 impurity and not S_2N_2 was made plain by the variability of its intensity with respect to those

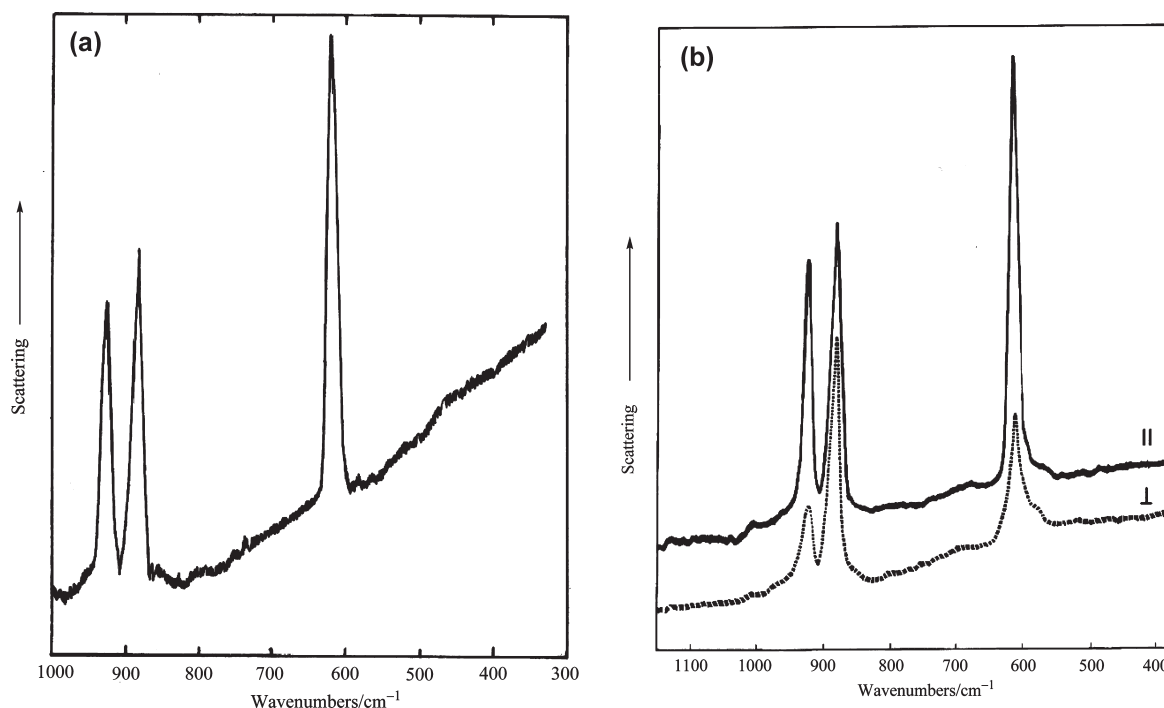


Figure 2. (a) Raman spectrum of a solid film of S_2N_2 at 20 K. (b) Raman spectrum of an N_2 matrix doped with S_2N_2 and showing the results of polarization measurements.

Table 4. Raman Spectrum of S_2N_2 in the Solid and Matrix-Isolated States (wavenumbers in cm^{-1})^a

annealed solid at 20 K	matrix at 20 K					assignment
	Ar:		Kr:	N ₂ :	CH ₄ :	
	$S_2^{14}N_2$	$S_2^{15}N_2$	$S_2^{14}N_2$	$S_2^{14}N_2$	$S_2^{14}N_2$	
924 s	934 s	902 s	926 s	929 s, p	928 s	$\nu_1 (a_g)$
884 ms	889 s	868 s	892 s	886 ms, dp	899 s	$\nu_3 (b_{1g})$
608 vs	617 vs	617 vs	617 vs	613 vs, p	621 vs	$\nu_2 (a_g)$

^a Intensities and states of polarization: s, strong; m, medium; v, very; p, polarized; dp, depolarized.

of the absorptions near 790 and 470 cm^{-1} and by its tracking another weak absorption near 2340 cm^{-1} attributable to ν_3 of CO_2 .³⁵ There remains the possibility that the impurity feature near 660 cm^{-1} could fortuitously have masked a weak band due to S_2N_2 , but there was no obvious way of settling the issue. What is certain, however, is that the b_{2u} mode of the isolated S_2N_2 molecule is very weak in IR absorption, a circumstance well-anticipated by the present and earlier¹⁷ DFT calculations.

The measured wavenumbers of the unique b_{1g} mode, ν_3 , of both $S_2^{14}N_2$ and $S_2^{15}N_2$ are of interest, since they permit an estimate of the S–N–S bond angle, α . On the basis of the G matrix elements listed by Lesiecki and Nibler³³ for the structurally analogous molecules Tl_2X_2 ($X = F$ or Cl), we may write for eq 2:

$$\frac{\nu_3^2}{\nu_3'^2} = \frac{\mu_S + \mu_N - (\mu_S - \mu_N)\cos\alpha}{\mu_S + \mu_N' - (\mu_S - \mu_N')\cos\alpha} \quad (2)$$

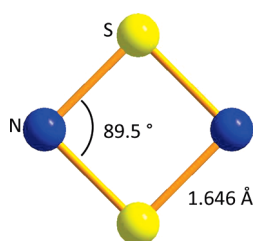
where the prime relates to $S_2^{15}N_2$ or ^{15}N and μ_X is the reciprocal mass of the atom X. Hence, α is calculated to be $89.1 \pm 1.5^\circ$, a value in close agreement with that of $89.58(6)^\circ$ determined for the molecule in the crystalline state and with the results of theoretical calculations. The error limits quoted refer to uncertainties in the measured wavenumbers but make no allowance for anharmonicity which is not expected greatly to affect the issue.

The Raman spectrum of solid S_2N_2 differs not at all from that of the matrix-isolated molecule in the number and relative intensities of the emissions and by no more than 10 cm^{-1} in their wavenumbers. Weaker features at low wavenumber were presumably obscured by the relatively high level of background scattering in the region of the Rayleigh line. The two IR absorptions near 790 and 470 cm^{-1} displayed by the matrix-isolated molecule are also reproduced closely in the spectrum of the crystalline solid. In this case, though, there is a significant difference in that the solid shows a band of medium intensity at 660.5 cm^{-1} . The most plausible interpretation is that this arises from the b_{2u} $\nu(S-N)$ fundamental, ν_5 , made more strongly active in IR absorption under the intermolecular interactions and/or the symmetry prevailing in the unit cell of the crystal. Vapor-grown S_2N_2 forms colorless monoclinic crystals with the space group $P2_1/c$ and two molecules per unit cell.^{6,10a} The structure reveals the herringbone pattern characteristic of molecular crystals with closest packing of planar molecules. The Bravais cell containing just two S_2N_2 molecules has effectively C_{2h} symmetry. Under these conditions, the internal vibrations of the molecules span the representation $3a_g + 3a_u + 3b_g + 3b_u$; the a_g and b_g modes correlate with the a_g and b_{1g} modes of the free molecule and are likewise active only in Raman scattering, while the a_u and b_u modes correlate with the b_{1u} , b_{2u} , and b_{3u} modes of the free molecule and match them in being active only in IR absorption.

Table 5. Vibrational Properties of S₂N₂ (wavenumbers and shifts in cm⁻¹, IR intensities and Raman activities relative to 100) Deduced from Quantum Chemical DFT Calculations^a

mode (irred rep)	IR intensity	Raman activity	wavenumbers for the isotopomers (experimental results)				isotopic shift relative to ³² S ₂ ¹⁴ N ₂ (experimental results)		
			³² S ₂ ¹⁴ N ₂	³² S ₂ ¹⁵ N ₂	³² S ₂ ¹⁴ N ¹⁵ N	³² S ³⁴ S ¹⁴ N ₂	³² S ₂ ¹⁵ N ₂	³² S ₂ ¹⁴ N ¹⁵ N	³² S ³⁴ S ¹⁴ N ₂
ν ₁ (a _g)	0	100	945.19 (934)	914.86 (902)	931.01	944.52	-30.33 (-32)	-14.18	-0.67
ν ₂ (a _g)	0	70	649.41 (617)	648.19 (617)	648.79	637.97	-1.22 (0)	-0.62	-11.44
ν ₃ (b _{1g})	0	54	926.09 (889)	904.48 (868)	915.60	921.99	-21.61 (-21)	-10.49	-4.1
ν ₄ (b _{1u})	46	0	482.04 (473.7)	470.73 (461.6)	476.42 (467.7)	479.88	-11.31 (-12.1)	-5.62 (-6.0)	-2.16
ν ₅ (b _{2u})	1	0	653.01	637.69	645.04	652.30	-15.32	-7.97	-0.71
ν ₆ (b _{3u})	100	0	795.50 (789.2)	776.84 (770.4)	785.20 (779.2)	791.81 (785.5)	-18.66 (-18.8)	-10.30 (-10.0)	-3.69 (-3.7)

^a B3LYP/6-311G++(3df,3pd): $F_{11} = 8.469$, $F_{22} = f_R = 6.573$, $F_{21} = 2f_{rR} = -5.109$, $F_{33} = f_r - f_{rr} - f_{rr}' + f_{rr}'' = 4.939$, $F_{44} = 2.666$, $F_{55} = f_r + f_{rr} - f_{rr}' - f_{rr}'' = 2.469$, $F_{66} = f_r - f_{rr} + f_{rr}' - f_{rr}'' = 3.599$; $f_r = 4.869$, $f_R = 6.573$, $f_{rR} = -2.554$, $f_{rr} = 0.600$, $f_{rr}' = 1.165$, $f_{rr}'' = 1.835$, $f_{oop} = 2.666$ mdyne Å⁻¹.

**Figure 3.** Molecular structure of S₂N₂ (*D*_{2h} symmetry).

That the spectra of the solid should resemble so closely those of the matrix-isolated molecules testifies to the molecular nature of the solid. Moreover, the absence from the solid spectra of measurable splitting in the bands due to internal vibrations of the molecules implies no more than weak intermolecular forces. In these circumstances, we see little alternative to assigning the IR absorption of the solid near 660 cm⁻¹ to the elusive b_{2u} mode, ν₅, and presume that this wavenumber differs but little from the value for the free molecule.

The other absorptions appearing in the IR spectrum of the solid—at 232 and 86 cm⁻¹—must then be due to intermolecular or lattice modes. The relatively high wavenumber of the first feature may be associated with a translator motion that involves stretching of the relatively short S...N contacts that occur along the *a*-axis of the crystal (measuring 2.890(1) Å as opposed to 3.35 Å for the sum of the relevant van der Waals radii).^{6,10a} This particular interaction may be seen to prefigure the course taken by subsequent polymerization to [SN]_x in which the *a*-axis of the S₂N₂ crystal transforms to the *b*-axis of the polymer.

On the basis of the spectra measured for matrix-isolated S₂N₂, we have carried out normal coordinate analysis calculations following the procedure described in the experimental section and drawing on the internal and symmetry coordinates adopted earlier for the analogous cyclic molecules Tl₂X₂³³ and Ge₂O₂.⁴³ The dimensions of the molecule were taken to be those measured experimentally for the crystalline solid, with *r*(S–N) = 1.654 Å and ∠NSN, α = 89.6° (see Figure 3). The resulting *F* matrix elements are given together with the calculated force constants in Table 6. The force field is found to reproduce well the wavenumbers of the different isotopomers of S₂N₂ isolated in an Ar matrix.

In its mapping of the global potential energy surface of a molecule, the vibrational force field provides through its

parameters an altogether more revealing and sensitive index to the bonding than do the bare dimensions. In the past, however, these parameters have too often been made relatively inaccessible by the need first to know the structure and dimensions of the molecule and/or by the lack of sufficient vibrational data to achieve a full solution of the relevant secular equation(s). Definitive structural information being in short supply in the early history of sulfur nitrides and their derivatives, recourse was frequently made to approximate S–N stretching force constants in correlations with both the length and order of S–N bonds.⁴⁴ These force constants were often based on relatively rudimentary force fields, being derived for the most part from the wavenumbers of the IR bands presumed to correspond to the S–N stretching fundamentals. The practical limitations of force constants as a guide to bonding have been alleviated by modern quantum chemical calculations that permit the routine simulation of not only the geometry but also a more or less realistic force field for molecules such as S₂N₂.

In Table 7 we compare the anharmonic S–N stretching force constant, *f*(SN), of S₂N₂ derived from normal coordinate analysis of the experimental spectra with the harmonic ones calculated by our DFT method [B3LYP/6-311G++(3df,3pd)]. Included in the same table are the corresponding details, as well as the S–N distances, *r*(SN), for some other sulfur–nitrogen compounds. Earlier studies have provided some or all of the relevant information for NSF₃,^{23,45} NS⁺X[−] (X[−] = [AsF₆][−], [SbF₆][−], or [Sb₂F₁₁][−]),^{23,46} NSF,^{23,47} NSCl,^{23,48} NS,^{23,49} [NS₂]⁺[SbCl₆][−],⁵⁰ NSH,^{51,52} HNS,^{51,52} FNSF₄,⁵³ S₄N₄,^{19,26d,38,54} S₄N₄H₄,⁵⁵ *trans*-H₂NSH,^{51,56} and N(SCF₃)₃.⁵⁷ We have supplemented these results with DFT calculations of the harmonic S–N stretching force constants for free NS⁺, NSF, NSH, HNS, S₄N₄, and *trans*-H₂NSH.

Overall, the results reveal the same sort of close inverse correlation between *f*(SN) and *r*(SN) that has been noted previously.⁴⁴ The molecules *trans*-H₂NSH,^{51,56} N(SCF₃)₃,⁵⁷ and S₄N₄H₄,⁵⁵ in which an S–N bond order of 1 might reasonably be assumed, are characterized by *r*(SN) = 1.67–1.72 Å and *f*(SN) = 3.4–4.0 mdyne Å⁻¹. It is true that an S–N σ-bond wholly free from any supplementary interaction is not easy to pin down. Thus, N(SCF₃)₃ has a planar NS₃ skeleton for which (p→d)π-bonding might once have been invoked.⁵⁷ While such an interaction must exist, its contribution to the bonding is now widely conceded to be relatively minor. HNS is perhaps the best and simplest candidate for a molecule with an S=N double bond; calculations indicate that it is characterized by *r*(SN) = 1.578 Å

Table 6. Vibrational Wavenumbers and Isotopic Splittings (in cm^{-1}) for the S_2N_2 Molecule from a Normal Coordinate Analysis Based on the Experimental Data

mode (irred. rep.)	isotopic shifts relative to $^{32}\text{S}_2^{14}\text{N}_2$					
	wavenumber		$^{32}\text{S}_2^{15}\text{N}_2$		$^{32}\text{S}_2^{14}\text{N}^{15}\text{N}$ (expt)	$^{32}\text{S}^{34}\text{S}^{14}\text{N}_2$ (expt)
	expt	calcd ^a	expt	calcd ^a		
ν_1 (a_g)	934	933.71	−32	−31.43	—	—
ν_2 (a_g)	617	617.25	0	−0.16	—	—
ν_3 (b_{1g})	889	888.93	−21	−20.86	—	—
ν_4 (b_{1u})	473.7	473.67	−12.1	−11.11	−6.0	—
ν_5 (b_{2u})	—	652.95	—	−15.23	—	—
ν_6 (b_{3u})	789.2	789.14	−18.8	−18.52	−10.0	−3.7

^a Details of **F** matrix and force constants: $F_{11} = 7.313$, $F_{22} = f_R = 6.763$, $F_{21} = 2f_{\text{rR}} = -4.837$, $F_{33} = f_r - f_{\text{rr}} - f_{\text{rr}}' + f_{\text{rr}}'' = 4.576$, $F_{44} = 2.575$, $F_{55} = f_r - f_{\text{rr}} + f_{\text{rr}}' - f_{\text{rr}}'' = 3.541$, $F_{66} = f_r + f_{\text{rr}} - f_{\text{rr}}' - f_{\text{rr}}'' = 2.455$; $f_r = 4.471$, $f_R = 6.763$, $f_{\text{rR}} = -2.419$, $f_{\text{rr}} = 0.413$, $f_{\text{rr}}' = 0.956$, $f_{\text{rr}}'' = 1.473$, $f_{\text{oop}} = 2.575$ mdyne \AA^{-1} .

Table 7. Valence Stretching Force Constants, $f(\text{SN})$ in mdyne \AA^{-1} , and SN Distances, $r(\text{SN})$ in \AA , in Selected SN Molecules

compd	normal coordinate analysis		theoretical calculations		ref
	$f(\text{SN})$	$r(\text{SN})$	$f(\text{SN})$	$r(\text{SN})$	
NSF_3	12.55	1.416			23, 45
NS^+	11.85	1.42	13.01 ^b	1.427	23, 46
NSF	10.71	1.448	11.54 ^b	1.440	23, 47
NSCl	10.10	1.450			23, 48
$\text{NS} (^2\Pi)$	8.53	1.496			23, 49
NS_2^+	8.26	1.463			50
NSH		1.509 ^a	8.16 ^b	1.494	51, 52
HNS		1.578 ^a	7.12 ^b	1.564	50, 51
FNSF_4	6.58	1.520			53
S_4N_4	5.05	1.623	4.70 ^d	1.623	19, 26d, 38, 54
S_2N_2	4.47	1.654	4.87 ^c	1.646	this work
$\text{S}_4\text{N}_4\text{H}_4$	4.01	1.67			55
$\text{trans-H}_2\text{NSH}$		1.719	3.95 ^b	1.720	49, 56
$\text{N}(\text{SCF}_3)_3$	3.40	1.70			57

^a Estimated by quantum chemical calculations; see ref 51. ^b This work; B3LYP/def2-TZVP valence force constant values obtained after transformation of the theoretically obtained Cartesian force constant matrix into a system of reasonable symmetry-adapted internal coordinates. ^c This work. ^d This work; B3LYP/def2-TZVP valence force constant values obtained after transformation of the theoretically obtained Cartesian force constant matrix into a system of reasonable internal coordinates. This set of internal coordinates is not symmetrized. It consists of the eight S–N bonds, the two S–S “bonds”, and eight S–S–N bending coordinates.

and a harmonic $f(\text{SN}) = 7.12$ mdyne \AA^{-1} .^{51,52} In the simplest sulfur nitride of all, the radical NS^\bullet with a bond order of 2.5, we find $r(\text{SN}) = 1.496$ \AA and $f(\text{SN}) = 8.53$ mdyne \AA^{-1} .^{23,49} A bond order of 3 is formally reached in the NS^+ cation with $r(\text{SN}) = 1.42$ \AA and $f(\text{SN}) = 11.85$ –13.01 mdyne \AA^{-1} .^{23,46}

Within this framework S_2N_2 with $r(\text{SN}) = 1.654$ \AA and $f(\text{SN}) = 4.47$ –4.87 mdyne \AA^{-1} emerges as having a bond order only slightly greater than 1. This implies that the 2π -electron aromaticity¹⁷ adds but little to the strength of what might be expected of the underlying σ -bonded skeleton. Interestingly, the bond order appears on the evidence of both $r(\text{SN})$ and $f(\text{SN})$ to be marginally lower than in the cage-like tetramer S_4N_4 ,^{19,26d,38,54} the historical and practical centerpiece to much of sulfur nitride chemistry.^{2–4} This may well reflect not so much the inherent strength of the S–N bonding as the ring strain in the four-membered S_2N_2 heterocycle. It is noteworthy, for example, that at 2.331 \AA the cross-ring $\text{N} \cdots \text{N}$ contact in S_2N_2 brings the N

atoms significantly closer together than in S_4N_4 , where the shortest contact measures 2.580 \AA .⁵⁴ $\text{N} \cdots \text{N}$ repulsion must therefore exert more influence in S_2N_2 than in S_4N_4 .

A different view of the S_2N_2 molecule is gained from the force constant f_{oop} defining resistance to out-of-plane deformation of the four-membered ring. Table 8 lists the **F** matrix elements and force constants for S_2N_2 alongside those for the structurally analogous molecules Si_2O_2 ,^{58,59} Ge_2O_2 ,⁴³ and Al_2Cl_2 ,⁶⁰ each containing two fewer valence electrons, the relevant details being determined either by normal coordinate analysis of experimental data or by DFT calculations. All of these molecules are in their ground electronic states; the case of P_2N_2 , also valence isoelectronic with Si_2O_2 , Ge_2O_2 , and Al_2Cl_2 , will be treated later. Here we note not only that the stretching force constant f_r decreases significantly in the order $\text{S}_2\text{N}_2 > \text{Si}_2\text{O}_2 > \text{Ge}_2\text{O}_2 \gg \text{Al}_2\text{Cl}_2$, but also that f_{oop} decreases even more precipitately in the same order. Thus f_{oop} for S_2N_2 is about 4 times greater than f_{oop} for Si_2O_2 and

Table 8. Comparison of the Symmetry and Internal Force Constants for the Molecules S_2N_2 , Si_2O_2 , Ge_2O_2 , and Al_2Cl_2 Derived from Experiment [normal coordinate analysis (nca)] and Theory [DFT calculations (B3LYP)]

F matrix element	S_2N_2		P_2N_2 : B3LYP ^{b,c}	Si_2O_2 : B3LYP ^c	Ge_2O_2		Al_2Cl_2 : B3LYP ^c
	nca	B3LYP ^a			nca ^d	B3LYP ^c	
$F_{11} = f_r + f_{rr} + f_{rr}' + f_{rr}''$	7.31	8.47	5.62	6.28	6.25	5.27	0.91
$F_{22} = f_R$	6.76	6.57	3.19	3.88	3.67	2.73	0.48
$F_{21} = 2f_{rR}$	−4.84	−5.11	−1.72	−2.84	−3.14	−2.20	−0.32
$F_{33} = f_r - f_{rr} - f_{rr}' + f_{rr}''$	4.57	4.94	3.55	1.80	1.63	1.42	0.10
$F_{44} = f_{oop}$ ^e	2.57	2.67	0.03	0.61	0.41	0.29	0.03
$F_{55} = f_r + f_{rr} - f_{rr}' - f_{rr}''$	2.46	2.47	3.03	3.75	3.01	3.29	0.62
$F_{66} = f_r - f_{rr} + f_{rr}' - f_{rr}''$	3.54	3.60	2.53	3.73	3.23	3.06	0.68
f_{rr}	0.413	0.600	0.641	1.125	1.103	1.021	0.190
f_{rr}'	0.956	1.165	0.394	1.116	1.209	0.903	0.217
f_{rr}''	1.473	1.835	0.902	0.150	0.411	0.086	−0.072
f_r	4.471	4.869	3.683	3.893	3.532	3.260	0.578
f_R	6.763	6.573	3.185	3.875	3.668	2.727	0.484
f_{rR}	−2.419	−2.554	−0.861	−1.422	−1.569	−1.100	−0.160
f_{oop}	2.575	2.666	0.03	0.610	0.414	0.289	0.029
R	N...N	N...N	N...N	O...O	O...O	O...O	Cl...Cl
other properties							
Q^f		S +0.57	P +0.13	Si +0.25		Ge +0.42	Al +0.14

^a B3LYP/6-311G++(3df,3pd). ^b Excited electronic state of P_2N_2 ; see the text and ref 59. ^c B3LYP/def2-TZVP. ^d Experimental force constants (see ref 43) after transformation (program FCT³²) based on internal coordinates using $R = O \cdots O$ and $\angle GeOGe = 94^\circ$. ^e $G_{44} = 1/2(\mu_1 + \mu_2)$; see the text. ^f Atomic charge obtained from population analysis calculations based on occupation numbers (Ahlrichs–Heinzmann population analysis²⁹).

nearly 2 orders of magnitude greater than f_{oop} for Al_2Cl_2 . In other words, S_2N_2 is a relatively rigid molecule whereas Si_2O_2 , Ge_2O_2 , and Al_2Cl_2 become increasingly floppy.

It is tempting to attribute the exceptional position of S_2N_2 to the 2π -electron aromaticity¹⁷ which is denied to the other molecules. However, there are other factors simultaneously at work, notably the charge separation between X and Y in these X_2Y_2 molecules. As the charge separation increases, so f_r and f_{oop} may be expected to decrease, and in the limit of a 100% ionic formulation, i.e., $X^+_2Y^-_{2,f_{oop}}$ actually tends to zero. Accordingly, we have drawn on population analysis calculations²⁹ to estimate the atomic charge Q for the more electropositive atom in each of these X_2Y_2 molecules, with the results given in Table 8. Somewhat surprisingly, the values of Q imply that the degree of charge separation decreases in the order $S_2N_2 > Ge_2O_2 > Si_2O_2 > P_2N_2 \sim Al_2Cl_2$.

P_2N_2 stands in contrast to all four of these molecules. Even though it has not been detected experimentally,⁵⁸ theoretical studies shed interesting light on the low-energy structures to which it has access.⁶¹ Perhaps the most striking point is that the lowest energy on the P_2N_2 potential energy surface is achieved not with a planar, cyclic structure with D_{2h} symmetry but with a closed-shell, butterfly-like one with C_{2v} symmetry, P–N bonds measuring 1.676 Å, with a fold angle of 149.5°. Among the other forms open to the molecule there is indeed a closed-shell D_{2h} isomer with $r(P-N) = 1.686$ Å and $\angle P-N-P = 63.7^\circ$, 133 kJ mol^{−1} higher in energy. This high-energy molecule is remarkable on two counts. First, it features an unusually short N...N contact of 1.779 Å, suggestive of either weak bonding or, more likely, a relatively strong repulsive interaction. Second, it is characterized by an out-of-plane deformation mode [ν_4 (b_{1u})]

calculated to be only 37 cm^{−1}.⁶¹ This suggests not only a high degree of pliancy along the relevant coordinate, but also through the second-order Jahn–Teller effect⁶² a route to stabilization of the molecule in a butterfly-like configuration.

Our own B3LYP-based DFT calculations give results entirely consistent with those of the earlier studies of P_2N_2 [made at the B3LYP/6-311+G(2df) and CASPT2(12e,12o)/ANO-L levels].⁶¹ For the higher energy D_{2h} form, for example, we find a geometry with $r(P-N) = 1.684$ Å, $r(N \cdots N) = 1.779$ Å, and $\angle N-P-N = 63.8^\circ$. The vibrational force field computed for this molecule, details of which are included in Table 8, is then noteworthy, as previously anticipated,⁵⁹ for an out-of-plane bending force constant, f_{oop} , of no more than 0.03 mdyne Å^{−1}. Like f_{oop} for Al_2Cl_2 , it is therefore some 2 orders of magnitude smaller than that for S_2N_2 . In the light of the calculated atomic charges, the values of f_{oop} run counter to the order of increasing charge separation. The obvious inference, therefore, to be drawn regarding the exceptional value of f_{oop} for S_2N_2 is that it does indeed reflect the restraining influence of the two extra electrons in a bonding π -type orbital. That the S–N bond order should appear, nevertheless, to be close to 1 raises the possibility of bonding featuring a relatively small σ - and a pronounced π -contribution.

5. CONCLUSIONS

The IR and Raman spectra of disulfur dinitride, S_2N_2 , isolated in a solid noble gas, N_2 , or CH_4 matrix at 20 K have been compared with those of the solid compound, the crystal structure of which has been determined previously.⁶ The results indicate that the isolated S_2N_2 molecule has essentially the same

geometry and dimensions as in the crystalline solid with a virtually square-planar ring conforming to D_{2h} symmetry, a conclusion confirmed by the response of the spectra to isotopic enrichment in ^{15}N , and by the results of earlier¹⁷ as well as fresh quantum chemical (DFT) calculations. Anharmonic and harmonic vibrational force fields have been calculated for S_2N_2 on the basis of a normal coordinate analysis of the experimental data and of DFT calculations [B3LYP/6-311G++(3df,3pd)], respectively. Hence the S–N stretching force constant, $f(\text{SN})$, in common with the S–N bond distance, $r(\text{SN})$, suggests a S–N bond order only marginally greater than 1 and slightly lower than that in the cage-like molecule S_4N_4 . By contrast, the unique out-of-plane deformation mode of the S_2N_2 molecule is characterized by a force constant, f_{oop} , markedly greater than those in the structurally analogous species Si_2O_2 , Ge_2O_2 , Al_2Cl_2 , and the high-energy D_{2h} isomer of P_2N_2 , each with two fewer valence electrons than the sulfur nitride. The greater rigidity of the S_2N_2 ring can most plausibly be linked to the two electrons occupying a π -type bonding orbital. This then leaves open to question the respective contributions to the S–N bonding made by σ - and π -type interactions, including the influence of the relatively large charge separation that apparently exists between the sulfur and nitrogen atoms.

■ ASSOCIATED CONTENT

S Supporting Information. Results of DFT quantum chemical calculations of the structures, energies, and vibrational properties of NS^+ , NSF , NSH , SNH , S_4N_4 , *trans*- H_2NSH , S_2N_2 , Si_2O_2 , Ge_2O_2 , Al_2Cl_2 , and D_{2h} isomer of P_2N_2 . This material is available free of charge via the Internet at <http://pubs.acs.org>.

■ AUTHOR INFORMATION

Corresponding Author

*E-mail: tony.downs@chem.ox.ac.uk.

■ ACKNOWLEDGMENT

One of us (S.C.P.) thanks the Science Research Council of the U.K. (SRC) for the award of a research fellowship, and another (R.E.) thanks Glen Creston for the funding of a research studentship. We thank the Steinbuch Centre of Computing of the Karlsruhe Institute of Technology for providing computational resources.

DEDICATION

[†]This paper is dedicated to Prof. Hansgeorg Schnöckel on the occasion of his 70th birthday and in recognition of his outstanding contributions to cluster chemistry, particularly touching the group 13 metals.

■ REFERENCES

- (1) Goehring, M.; Voigt, D. *Naturwissenschaften* **1953**, *40*, 482.
- (2) (a) Becke-Goehring, M. *Quart. Rev. (London)* **1956**, *10*, 437. (b) Becke-Goehring, M. *Prog. Inorg. Chem.* **1959**, *1*, 207.
- (3) (a) Heal, H. G. *The Inorganic Heterocyclic Chemistry of Sulfur, Nitrogen and Phosphorus*; Academic Press: London, U.K., 1980. (b) Woollins, J. D. *Non-Metal Rings, Cages and Clusters*; Wiley: Chichester, U.K., 1988. (c) Chivers, T. *A Guide to Chalcogen-Nitrogen Chemistry*; World Scientific Publishing Co.: Singapore, 2004. (d) Chivers, T.; Manners, I. *Inorganic Rings and Polymers of the p-Block Elements: From*

Fundamentals to Applications; RSC Publishing: Cambridge, U.K., 2009; Chapter 12.

- (4) (a) Greenwood, N. N.; Earnshaw, A. *Chemistry of the Elements*, 2nd ed.; Butterworth-Heinemann: Oxford, U.K., 1997. (b) Holleman, A. F.; Wiberg, E.; Wiberg, N. *Inorganic Chemistry*; Academic Press: San Diego, CA, 2001; pp 559–572.
- (5) Patton, R. L.; Raymond, K. N. *Inorg. Chem.* **1969**, *8*, 2426.
- (6) Mikulski, C. M.; Russo, P. J.; Saran, M. S.; MacDiarmid, A. G.; Garito, A. F.; Heeger, A. J. *J. Am. Chem. Soc.* **1975**, *97*, 6338.
- (7) Roemmele, T. L.; Konu, J.; Boeré, R. T.; Chivers, T. *Inorg. Chem.* **2009**, *48*, 9454.
- (8) See, for example, Banister, A. J.; Gorrell, I. B. *Adv. Mater.* **1998**, *10*, 1415 and references cited therein.
- (9) Mawhinney, R. C.; Goddard, J. D. *J. Mol. Struct. (THEOCHEM)* **2008**, *856*, 16.
- (10) (a) Cohen, M. J.; Garito, A. F.; Heeger, A. J.; MacDiarmid, A. G.; Mikulski, C. M.; Saran, M. S.; Kleppinger, J. *J. Am. Chem. Soc.* **1976**, *98*, 3844. (b) Baughman, R. H.; Chance, R. R.; Cohen, M. J. *J. Chem. Phys.* **1976**, *64*, 1869. (c) Müller, H.; Svensson, S. O.; Birch, J.; Kvik, Å. *Inorg. Chem.* **1997**, *36*, 1488. (d) Mawhinney, R. C.; Goddard, J. D. *Inorg. Chem.* **2003**, *42*, 6323.
- (11) Kelly, P. F.; King, R. S. P.; Mortimer, R. J. *Chem. Commun.* **2008**, 6111.
- (12) (a) Adkins, R. R.; Turner, A. G. *J. Am. Chem. Soc.* **1978**, *100*, 1383. (b) Jafri, J. A.; Newton, M. D.; Pakkanen, T. A.; Whitten, J. L. *J. Chem. Phys.* **1977**, *66*, 5167.
- (13) (a) Skrezenek, F. L.; Harcourt, R. D. *J. Am. Chem. Soc.* **1984**, *106*, 3934. (b) Harcourt, R. D.; Skrezenek, F. L. *J. Mol. Struct. (THEOCHEM)* **1987**, *151*, 203. (c) Harcourt, R. D.; Klapötke, T. M.; Schulz, A.; Wolyne, P. *J. Phys. Chem. A* **1998**, *102*, 1850. (d) Klapötke, T. M.; Li, J.; Harcourt, R. D. *J. Phys. Chem. A* **2004**, *108*, 6527.
- (14) Gerratt, J.; McNicholas, S. J.; Karadakov, P. B.; Sironi, M.; Raimondi, M.; Cooper, D. L. *J. Am. Chem. Soc.* **1996**, *118*, 6472.
- (15) Jung, Y.; Heine, T.; Schleyer, P. v. R.; Head-Gordon, M. *J. Am. Chem. Soc.* **2004**, *126*, 3132.
- (16) Tuononen, H. M.; Suontamo, R.; Valkonen, J.; Laitinen, R. S. *J. Phys. Chem. A* **2004**, *108*, S670.
- (17) Tuononen, H. M.; Suontamo, R.; Valkonen, J.; Laitinen, R. S.; Chivers, T. *J. Phys. Chem. A* **2005**, *109*, 6309.
- (18) Warn, J. R. W.; Chapman, D. *Spectrochim. Acta* **1966**, *22*, 1371.
- (19) Bragin, J.; Evans, M. V. *J. Chem. Phys.* **1969**, *51*, 268.
- (20) (a) Frost, D. C.; LeGeyt, M. R.; Paddock, N. L.; Westwood, N. P. C. *J. Chem. Soc., Chem. Commun.* **1977**, 217. (b) Findlay, R. H.; Palmer, M. H.; Downs, A. J.; Egdel, R. G.; Evans, R. *Inorg. Chem.* **1980**, *19*, 1307.
- (21) Jolly, W. L.; Becke-Goehring, M. *Inorg. Chem.* **1962**, *1*, 76.
- (22) (a) Becke-Goehring, M. *Inorg. Synth.* **1960**, *6*, 123. (b) Douillard, A.; May, J.-F.; Vallet, G. C. R. *Seances Acad. Sci., Ser. C* **1969**, *269*, 212.
- (23) Peake, S. C.; Downs, A. J. *J. Chem. Soc., Dalton Trans.* **1974**, 859.
- (24) Logan, N.; Jolly, W. L. *Inorg. Chem.* **1965**, *4*, 1508.
- (25) Hawkins, M.; Downs, A. J. *J. Phys. Chem.* **1984**, *88*, 1527, 3042.
- (26) (a) Downs, A. J.; Hawkins, M. *Adv. Infrared Raman Spectrosc.* **1983**, *10*, 1. (b) Burdett, J. K.; Downs, A. J.; Gaskill, G. P.; Graham, M. A.; Turner, J. J.; Turner, R. F. *Inorg. Chem.* **1978**, *17*, 523. (c) Hawkins, M. D. Phil. Thesis, University of Oxford, U.K., 1981. (d) Evans, R. Ph.D. Thesis, University of Oxford, U.K., 1980.
- (27) (a) Becke, A. D. *J. Chem. Phys.* **1993**, *98*, 564. (b) Lee, C.; Yang, W.; Parr, R. *Phys. Rev. B* **1988**, *37*, 785.
- (28) Weigend, F.; Ahlrichs, R. *Phys. Chem. Chem. Phys.* **2005**, *7*, 3297.
- (29) (a) Heinzmann, R.; Ahlrichs, R. *Theor. Chim. Acta* **1976**, *42*, 33. (b) Davidson, E. R. *J. Chem. Phys.* **1967**, *46*, 3320. (c) Roby, K. R. *Mol. Phys.* **1974**, *27*, 81.
- (30) Ahlrichs, R.; Bär, M.; Häser, M.; Horn, H.; Kölmel, C. *Chem. Phys. Lett.* **1989**, *162*, 165.

- (31) Deglmann, P.; Furche, F.; Ahlrichs, R. *Chem. Phys. Lett.* **2002**, 362, 511.
- (32) Pulay, P. Program for the transformation of force constants FCT, private communication.
- (33) Lesiecki, M. L.; Nibler, J. W. *J. Chem. Phys.* **1975**, 63, 3452.
- (34) Hedberg, L.; Mills, I. M. *J. Mol. Spectrosc.* **1993**, 160, 117.
- (35) See, for example, the following and references cited therein:
- (a) Kukolich, S. G. *J. Am. Chem. Soc.* **1982**, 104, 4715. (b) McKellar, A. R. W.; Watson, J. K. G.; Howard, B. J. *Mol. Phys.* **1995**, 86, 273.
- (c) Brookes, M. D.; McKellar, A. R. W.; Amano, T. *J. Mol. Spectrosc.* **1997**, 185, 153. (d) Krim, L. *J. Mol. Struct.* **1998**, 471, 267.
- (36) Somasundram, K.; Handy, N. C. *J. Phys. Chem.* **1996**, 100, 17485.
- (37) Bridgeman, A. J.; Cunningham, B. *Spectrochim. Acta, Part A* **2004**, 60, 471.
- (38) Turowski, A.; Appel, R.; Sawodny, W.; Molt, K. *J. Mol. Struct.* **1978**, 48, 313.
- (39) (a) Nelson, J.; Heal, H. G. *J. Chem. Soc. A* **1971**, 136. (b) Chivers, T.; Coddling, P. W.; Laidlaw, W. G.; Liblong, S. W.; Oakley, R. T.; Trsic, M. *J. Am. Chem. Soc.* **1983**, 105, 1186.
- (40) (a) Mikulski, C. M.; Russo, P. J.; Saran, M. S.; MacDiarmid, A. G.; Garito, A. F.; Heeger, A. J. *J. Am. Chem. Soc.* **1975**, 97, 6358. (b) Stolz, H. J.; Wendel, H.; Otto, A.; Pintschovius, L.; Kahlert, L. *Phys. Status Solidi B* **1976**, 78, 277. (c) Macklin, J. W.; Street, G. B.; Gill, W. D. *J. Chem. Phys.* **1979**, 70, 2425. (d) Kanazawa, H.; Stejny, J.; Keller, A. *J. Mater. Sci.* **1990**, 25, 3838.
- (41) (a) Ayers, G. P.; Pullin, A. D. E. *Spectrochim. Acta, Part A* **1976**, 32, 1629. (b) Fredin, L.; Nelander, B.; Ribbegård, G. *J. Mol. Spectrosc.* **1974**, 53, 410. (b) Guasti, R.; Schettino, V.; Brigot, N. *Chem. Phys.* **1978**, 34, 391.
- (42) (a) Fredin, L.; Nelander, B.; Ribbegård, G. *J. Mol. Spectrosc.* **1974**, 53, 410. (b) Guasti, R.; Schettino, V.; Brigot, N. *Chem. Phys.* **1978**, 34, 391.
- (43) Zumbusch, A.; Schnöckel, H. *J. Chem. Phys.* **1998**, 108, 8092.
- (44) See, for example, (a) Goubeau, J. *Angew. Chem., Int. Ed. Engl.* **1966**, 5, 567. (b) Siebert, H. *Anwendungen der Schwingungsspektroskopie in der Anorganischen Chemie*; Springer-Verlag: New York, 1966; Glemser, O.; Müller, A.; Böhler, D.; Krebs, B. *Z. Anorg. Allg. Chem.* **1968**, 357, 184.
- (45) Sawodny, W.; Fadini, A.; Ballein, K. *Spectrochim. Acta* **1965**, 21, 995.
- (46) Glemser, O.; Koch, W. *Angew. Chem., Int. Ed. Engl.* **1971**, 10, 127. Clegg, W.; Glemser, O.; Harms, K.; Hartmann, G.; Mews, R.; Noltemeyer, M.; Sheldrick, G. M. *Acta Crystallogr.* **1981**, B37, 548.
- (47) Kirchhoff, W. H.; Wilson, E. B., Jr. *J. Am. Chem. Soc.* **1963**, 85, 1726. Mirrl, A. M.; Guarnieri, A. *Spectrochim. Acta* **1967**, 23A, 2159.
- (48) Beppn, T.; Hirota, E.; Morino, Y. *J. Mol. Spectrosc.* **1970**, 36, 386.
- (49) Lide, D. R., Ed. *Handbook of Chemistry and Physics*, 90th ed.; CRC Press: Boca Raton, FL, 2009–2010.
- (50) Silaghi-Dumitrescu, I.; Haiduc, I. *J. Mol. Struct. (THEOCHEM)* **1984**, 106, 217.
- (51) Pereira, P. S. S.; Macedo, L. G. M.; Pimentel, A. S. *J. Phys. Chem. A* **2010**, 114, 509.
- (52) Denis, P. A.; Ventura, O. N.; Mai, H. T.; Nguyen, M. T. *J. Phys. Chem. A* **2004**, 108, 5073.
- (53) DesMarteau, D. D.; Eysel, H. H.; Oberhammer, H.; Günther, H. *Inorg. Chem.* **1982**, 21, 1607.
- (54) Almond, M. J.; Forsyth, G. A.; Rice, D. A.; Downs, A. J.; Jeffery, T. L.; Hagen, K. *Polyhedron* **1989**, 8, 2631.
- (55) Steudel, R.; Rose, F. *Spectrochim. Acta* **1977**, 33A, 979.
- (56) Lovas, F. J.; Suenram, R. D.; Stevens, W. J. *J. Mol. Spectrosc.* **1983**, 100, 316.
- (57) Bürger, H.; Pawelke, G.; Haas, A.; Willner, H.; Downs, A. J. *Spectrochim. Acta* **1978**, 34A, 287.
- (58) Schnöckel, H.; Mehner, T.; Plitt, H. S.; Schunck, S. *J. Am. Chem. Soc.* **1989**, 111, 4578.
- (59) Friesen, M.; Junker, M.; Zumbusch, A.; Schnöckel, H. *J. Chem. Phys.* **1999**, 111, 7881.
- (60) (a) Schnöckel, H. *Z. Naturforsch. B* **1976**, 31, 1291. (b) Himmel, H.-J. *Eur. J. Inorg. Chem.* **2005**, 1886.
- (61) Kwon, O.; Almond, P. M.; McKee, M. L. *J. Phys. Chem. A* **2002**, 106, 6864.
- (62) See, for example: Burdett, J. K. *Chemical Bonds: A Dialog*; Wiley: Chichester, U.K., 1997.